Energy & Environmental Science

Accepted Manuscript

ROYAL SOCIETY OF CHEMISTRY

www.rsc.org/ees

Journal Name

RSCPublishing

COMMUNICATION

Investigating charge dynamics in halide perovskite-sensitized mesostructured solar cells.

Cite this: DOI: 10.1039/xoxxoooooox

V. Roiati [a,b,c,†] S. Colella[d,†] G. Lerario,[a] L. De Marco,[a] A. Rizzo,[d] A. Listorti* [a, d] and G. Gigli[a,d,e]

Received ooth January 2012,
Accepted ooth January 2012

DOI: 10.1039/xoxxoooooox

www.rsc.org/

Charge generation and transport in $(CH_3NH_3)PbI_{3-x}Cl_x$ sensitized mesostructured solar cells are investigated. Highly efficient charge generation is directly proved by time correlated single photon counting analysis. Photoinduced absorption and transient photovoltage investigations depict double charge recombination dynamics. To explain the high device performances according to those spectroscopic observations, we suggest the existence of two complementary paths for electron transport, involving either TiO_2 and perovskite matrixes.

Sensitized solar cells, among the alternatives to silicon-based photovoltaic devices, harnesses great interest for their potentially easy processability, roughness, efficiency and low production costs.[1] However these devices, for diverse reasons, have been encountering difficulties in reaching the stage of a technological transfer.[2,3] The presence of a liquid corrosive electrolyte in the classical Dye Sensitized Solar Cells (DSSCs) or the still limited efficiencies reached by solid sensitized solar cells, have been the main obstacles for this scale up. Starting from 2012 the utilization in full solid sensitized devices of an underexplored eclectic class of materials, hybrid halide perovskites, has signified a field breakthrough allowing novel device layouts leading to record performances,[4–8] holding the promise of cost effective solar energy production. The utilization of these hybrid materials offers both the advantages of the organic compounds, such as solution processability and optical properties tunability, and those of the inorganic crystalline semiconductors, like high charge mobilities and large absorption coefficients. This class of materials has been firstly investigated many years ago, but they have never been employed as active components in solar converting devices before 2009.[9–14] For this reason, despite the widening literature on the subject, many questions, concerning their peculiar structural chemistry and the physics of light induced processes have to be addressed, foreseeing further advancements on this emerging research front. Perovskite can act as a sensitizing layer deposited on a mesostructured semiconductor such as TiO_2,[6,13–17] as p-type material in a depleted hole conductor-free heterojunction solar cells[18,19] or as n-type light harvesting and charge transporting material, layered on an inert mesostructured oxide (Al_2O_3) and coupled with a Hole Transporting Material (HTM).[5,20] Even though a detailed rationalization of the charge generation and transport for all of these architectural diverse devices has not been yet carried out, the ability of perovskite to efficiently perform ambipolar charge transport implies a peculiar mechanism with respect to the conventional solid sensitized solar cells. An important question to be addressed regards the interpretation of the perovskite's behaviour when sandwiched between a n-type and a p-type material. In this scenario, in fact, it could contribute to the transport of either electrons or holes and constitute in this way an alternative path for charge collection. This possibility, to the best of our knowledge, has not been directly investigated or proven so far. Here we propose a picture for charge generation and recombination in **$(CH_3NH_3)PbI_{3-x}Cl_x$** (**PERO** in the paper) solar cells employing TiO_2 as mesoporous substrates and spiro-OMeTAD as HTM. Time correlated single photon counting (TCSPC),[21–23] photoinduced absorption (PIA) and transient photocurrent/photovoltage (TPC/TPV) measurements,[24–27] were selected as direct investigative tools for the determination of charge generation and transport in model systems and working devices. The collection of our results depicts a peculiar unusual behaviour for charge dynamics, as the presence of two n-type materials, TiO_2 and perovskite, generates alternative paths for electron transport. This important new insight would help the comprehension of these innovative devices suggesting potential design improvements.

Throughout the report we compared a **PERO**-based device with a solid-state sensitized solar cell manufactured employing a well know organic dye: **D149**. Our aim, in fact, is to compare the photo-physical processes taking place in **PERO**-sensitized cell with that of a device with comparably thin photoanode and high efficiency in charge density generation.[28] Device preparation details are reported in Supporting Information, while photovoltaic performances of **PERO** and **D149** in a SS-DSSC are resumed in Figure 1.

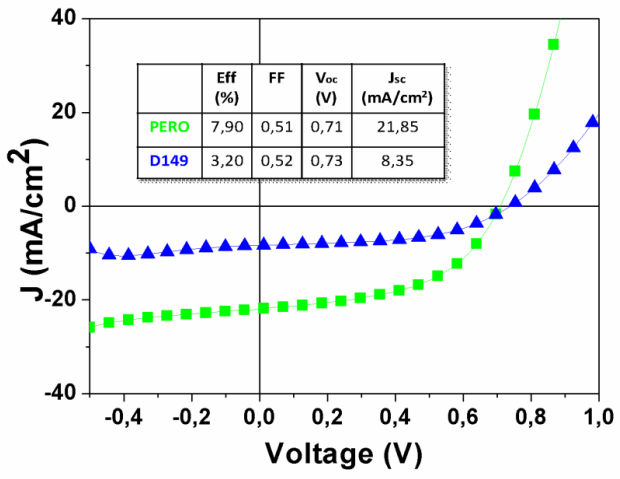

Fig. 1. a) Light J-V curves for **PERO** and **D149** based devices and the corresponding photovoltaic parameters (inset).

The remarkable difference in power conversion efficiency (PCE) between the organic dye and the perovskite, 3,2% and 7,9% respectively, was essentially due to the improved photocurrent, almost three-fold higher, which characterizes the hybrid compound. The short-circuit current (J_{sc}) largely depends on the photogenerated carriers and on the interfacial recombination of the electrons and holes. The large difference found for the two compounds can be ascribed to the perovskite absorption extension, toward near infrared region, with respect to the organic dye, as clearly seen by comparing the absorption spectra and the IPCE of the two devices in Figure S1 (Supporting Information).

Monochromatic time resolved photoluminescence (TRPL) was collected with a custom-made time correlated single photon counting (TCSPC). This is a standard procedure for the determination of the charge generation efficiency in liquid and solid DSSC or nano crystal sensitized solar cells.[19,20,22] The technique is based on the comparison between the photoluminescence (PL) decay of the sensitizer embedded in a working device and in a reference system, in which the presence of an inert substrate is preventing the charge extraction. [29,30] Very recently this methodology has been employed for the determination of excitons and/or electron-hole diffusion length in perovskite based solar cells. In both these pioneering reports the PL-quenching has been associated with the charge extraction in systems containing a perovskite flat thin layer, coupled with diverse charge extracting materials: n-type such as PCBM or p-type such as Spiro-OMeTAD.[31,32] Here we employed the same methodology to investigate mesostructured devices based on perovskite sensitizers combining TiO_2 matrix and Spiro-OMeTAD as n-type and p-type materials, respectively. Five model samples were manufactured, listed in Table 1, with the intention of separately investigate the active interfaces, with the exception of Sample 5 which corresponds to a working solar cell, bearing both TiO_2/**PERO** and **PERO**/HTM interfaces.

Figure 2 shows TCSPC luminescence decays collected on the maximum of the **PERO** emission, for 4 of the 5 model samples described in Table 1.

Table 1. Investigated samples description. (TCO = transparent conductive oxide; CL = TiO_2 compact layer; PMMA = polymethylmethacrylate).

Sample	Sample architecture
1	Glass/**PERO**/PMMA
2	Glass/Al_2O_3/**PERO**/PMMA
3	TCO/CL/TiO_2/**PERO**/PMMA
4	TCO/CL/Al_2O_3/**PERO**/Spiro-OMeTAD
5	TCO/CL/TiO_2/**PERO**/Spiro-OMeTAD/Ag

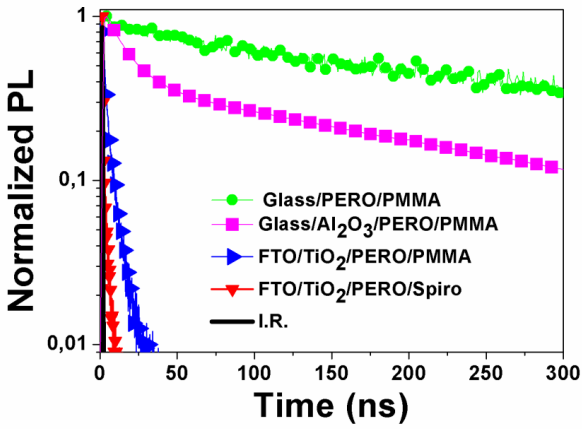

Fig. 2. Time-correlated-single-photon-counting (TCSPC) luminescence decays for samples 1-2-3-5 of Table 1. PL is collected at 770 nm, exciting with 635 nm ps pulsed laser. Instrumental response is also reported (100 ps FWHM). Exponential decays have been fitted with exponential functions (single or double) giving the following lifetimes: 350 ns for Glass/**PERO**/PMMA; 20 and 320 ns for Al_2O_3/**PERO**/PMMA; 4 ns for TiO_2/**PERO**/PMMA and 2 ns for TiO_2/**PERO**/Spiro-OMeTAD.

Comparing PL decay of TiO_2/**PERO**/PMMA and TiO_2/**PERO**/Spiro with the one of Glass/**PERO**/PMMA, our reference, we can observe that the charge generation in these systems is extremely efficient as reported and discussed in recent reports.[31–33] A very interesting and unusual observation arises from the comparison between **PERO** PL decay in Glass/**PERO**/PMMA and Al_2O_3/**PERO**/PMMA, which are supposed to give comparative results as in both cases the sensitizer is sandwiched between substrates preventing the charge extraction from the perovskite film. However the PL is reasonably quenched, showing a fast component of 20 ns, even when perovskite is deposited on Al_2O_3. An interesting debate concerning the fate of perovskite-excited states is occurring within the scientific community. Up to now, population of free charges and loosely bound excitons has been hypothesized to coexist in dynamic equilibrium established after the light absorption.[31] Coupling perovskite with diverse active materials, a PL quenching was observed and related to the charge extraction, however we found here that it could also occur in systems where injection cannot take place, and in these cases it could most likely be caused by oxide/perovskite interfacial interactions, as we further discuss and prove throughout the paper.

To directly monitor charge extraction in the investigated systems we performed continuous wavelength (cw) Photo-Induced Absorption (PIA). In cw-PIA an on/off monochromatic continuum laser source provides the excitation flux while a white light probes the photo-generated species. Formation and recombination of charge carriers is monitored in the µs-ms time domain. This spectroscopic tool is widely used for the determination of the charge generation efficiency in both liquid (LE-) DSSC and solid (SS-) DSSC.[26,5,34] In figure 3a we compare the PIA spectrum of Sample 3 of the initial set with a system containing **D149** sensitizer replacing **PERO**.[25] The broad negative signal assigned to the (TiO_2) electrons is almost two orders of magnitude smaller in the case of **PERO** compared to **D149**. Noticeably the feature is symmetrically present both in the in-phase and out-of-phase signal (see Figure S2) and this is a recognized fingerprint of long living species. This peculiar observation can be correlated with the TCSPC measurements. PL quenching for TiO_2/**PERO** systems, as in the previously discussed case of Al_2O_3/**PERO**, would not be straightforwardly related to a charge extraction, but the exciton dissociation leading to charge generation could occur within the perovskite layer in presence of an active interface. As a consequence, the weak electron PIA signal along with very efficient PL quenching can likely be explained by hypothesizing the formation of a charge reservoir within the perovskite layer at the interface with TiO_2. Noticeably a similar deduction has been drawn for $CH_3NH_3I_3$ perovskite sensitizer by means of Electrochemical Impedance Spectroscopy (EIS) measurements,[35] supporting our hypothesis. Steady state photoluminescence of **PERO** (peaking at 770 nm) and of **D149** (peaking at 600 nm) are also reported in figure.

In Figure 3a we attribute the positive feature peaking around the onset of perovskite absorption (765 nm) to the ground state absorption bleaching,[31,32] in fact it partially disappears when Spiro-OMeTAD is present and regenerates the oxidized perovskite (see Figure 2b). Contrarily the negative shoulder peaked at 720 nm is still observed after regeneration. The peculiar shape of the two features, together with the considerable amplitude of the positive peak, might reveal a contribution from Stark effect superimposed to the PIA signal.[34,36] This interesting observation, related to the presence of local electric field affecting molecular electronic transitions, could help in rationalizing the charge distribution at the various interfaces of perovskite-based devices therefore will be object of quantitative investigations.[37] In Figure 3b strong oxidized Spiro-OMeTAD features can be observed in the near infrared (NIR) region between 1000 and 1400 nm for both sample 4 (Al_2O_3/**PERO**/Spiro-OMeTAD) and 5 (TiO_2/**PERO**/Spiro-OMeTAD), with intensities in accordance with reported efficient hole transfer to this HTM.[25,38] The spectra in figure 3b clearly show differences in two regions: between 850 nm and 1000 nm where the absorption of injected electrons in the TiO_2 device is observable, while no photo-generated species are present in the case of inert scaffold Al_2O_3, and in the NIR region (1200-1600 nm) where the presence of such injected electrons shifts the positively charged Spiro-OMeTAD attributable features, towards longer wavelengths.[38,25]

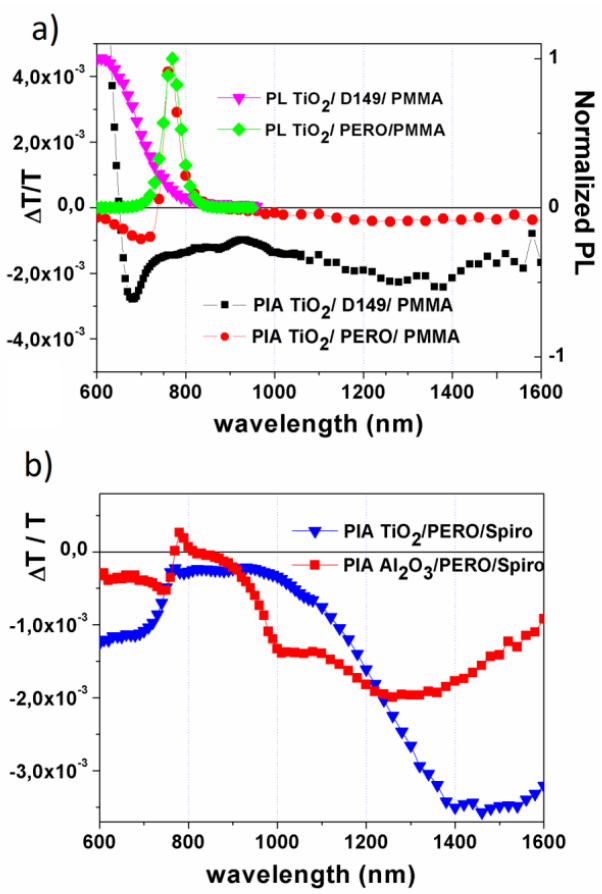

Fig. 3. a) Photoinduced absorption (PIA) and steady state photoluminescence (PL) spectra of TiO_2 thin films sensitized with **PERO** and **D149** covered with thin PMMA insulating layers. **PERO PIA** spectrum has 10X magnification. b) Photoinduced absorption (PIA) spectra for TiO_2 and Al_2O_3 thin films sensitized with **PERO** covered with films of Spiro-OMeTAD HTM.

In order to further rationalize transport and recombination mechanisms in our devices we performed transient photovoltage (TPV) and photocurrent (TPC, Figure S3) measurements. These techniques are widely employed for the determination of electron lifetimes (τ_e) in DSSCs. For a cell held at open circuit (V_{oc}) the carriers concentration in the charge-transporting matrix is varied by applying a tunable bias light, while a short weak pulse determines an additional amount of generated charge. The transient photovoltage associated with this population perturbation is related to electron recombination processes.[24,27] The extracted τ_e is shown, in Figure 4, as a function of the open-circuit voltage on complete working devices. Electron recombination lifetime is calculated fitting the transient photovoltage decay with single or double exponential functions, depending on the sample, as clarified in the results discussion. In this case the TiO_2/**PERO**/Spiro-OMeTAD device (Sample 5) is compared with a conventional liquid LE-DSSC: TiO_2/**D149**/Iodine-based electrolyte, and a solid state SS-DSSC: TiO_2/**D149**/Spiro-OMeTAD,[21,25] both bearing the same dye, with the intention of comparing the kinetics as function of the charge generation/recombination mechanisms involved. The decrease in τ_e at higher open circuit voltage is attributed to relatively faster recombination. This is usually observed in DSSCs and it is caused

by the increased concentration of electrons in TiO_2 conduction band at higher light intensity and device potential.

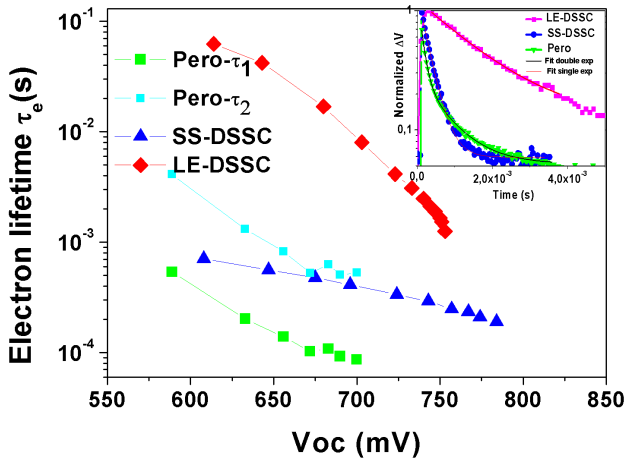

Fig. 4. Electron lifetime as a function of open circuit voltage, derived from exponential fitting of transient photovoltage decays at modulated light intensity. Three sensitized solar cells are compared: conventional liquid electrolyte (LE) dye sensitized solar cell (DSSC): TiO_2/**D149**/iodine based electrolyte (red, rhombus), solid state SS-DSSC: TiO_2/**D149**/Spiro-OMeTAD (blue, triangles) and the perovskite solar cell: TiO_2/**PERO**/Spiro-OMeTAD (green, squares; cyan, small squares). For perovskite-based solar cell we reported on the graph both the fast and the slow components of the transient photovoltage decay fitting. Inset: Normalized transient photovoltage curves at V_{oc} TiO_2/**D149**/iodine based electrolyte (red), TiO_2/**D149**/Spiro-OMeTAD (blue) and TiO_2/**PERO**/Spiro-OMeTAD (green).

Electron lifetimes for the devices under examination are found to be noticeably different along the series. The mechanism for the electron capturing in LE-DSSCs involves multi electron processes and it is known to be much slower than in solid-state devices.[27] The two solid state solar cells differs only for the presence of the perovskite layer replacing the organic dye in between TiO_2 and HTM, therefore perovskite is likely playing an active role in the recombination dynamics. Interestingly the perovskite-based device TiO_2/**PERO**/Spiro-OMeTAD is the only device for which the transient photovoltage decay is well fitted by a bi-exponential curve (see inset figure 4) instead of a single exponential. This observation suggests the presence of two distinguished populations of generated carries, recombining independently. The charge population bearing long lifetime is attributable to the electrons transported through the TiO_2 matrix to the FTO anode. Two evidences support this consideration: first, its coincidence with the curve of SS-DSSC reference,[39] and, second, the complete PIA spectrum showing a weak long living signal attributable to the TiO_2 electrons (see S2 figure already discussed above and S3). The fast component is the fastest decay observed for the investigated set, more than two orders of magnitude faster than the LE-DSSC and about one order of magnitude comparing it with the SS-DSSC. We associate this component to the charge confined within the perovskite layer recombining with holes in HTM. This attribution is based on the interconnection of all the previous observations: a high PL quenching leading to high charge generation, associated, however, to a very small TiO_2 electron absorption in the PIA analysis. Thus to justify the high device performances, carries are required to reach the FTO electrode within the perovskite itself. Furthermore, we highlight that the charge collection dynamic needs to be very fast in order to assure high device performances, considering the high recombination rates deduced from TPV. Such fast transport, already remarked by other recent investigations,[5,40] has been proved with transient photocurrent measurement (see Figure S4). The peculiar combination of short recombination lifetime and fast transport assure high collection efficiency and so good device performances. TiO_2/Perovskite interface in HTM-free devices has recently been rationalized with the formation of a depletion layer[19] The collection of our results, depicts, however, a peculiar unusual behavior for charge dynamics in perovskite-sensitized solar cells bearing spiro-OMeTAD as hole conductor. The presence of two n-type materials in the system, TiO_2 and perovskite, generates alternative paths for electron transport, compatible with the formation of a charge accumulation layer in the perovskite film, recently proved for similar device layout by Kim et al..[35] Further studies need to focus on the nature of this interface transport layer and on the mechanisms through which charge is transported within it.

Conclusions

In summary, $(CH_3NH_3)PbI_{3-x}Cl_x$ perovskite coupled with TiO_2 mesoporous substrate and Spiro-OMeTAD as solid state hole transporting material was spectroscopically investigated. Time correlated single photon counting proved efficient PL quenching for **PERO** deposited on TiO_2 and fast **PERO**/HTM hole transfer. We demonstrated that efficient PL quenching in these devices, is not straightforwardly related to electron injection in the TiO_2, as commonly occurring for solid state DSSCs, but can additionally be caused by oxide/perovskite interactions. Photoinduced absorption and transient photovoltage performed on working devices, in fact, described a double charge recombination dynamic that we attribute to the existence of an electron percolation channel present within the perovskite film, alternative to the TiO_2 mediated collection. The two paths are proved to complementary contribute to the photocurrent as demonstrated by the high efficiency obtained for **PERO**-based device. The proposed model for charge collection mechanism in perovskite mesostructured devices would prefigure experimental findings not aligned with those expected for classical SS-DSSCs, highlighting the need of a specific approach to systems including those material both in term of data interpretation and device development.

Acknowledgments

This work was supported by EFOR-CNR, by PON-MAAT (Project Number: PON02_00563_3316357), by PON-FORM@BEYOND-NANO. The authors gratefully acknowledge Dr. Michele Manca, Dr. Milena De Giorgi, Mr. Paolo Cazzato and Dr. Marco Mazzeo for fruitful discussion and technical support.

Notes and references

[a] Center for Bio-Molecular Nanotechnology - Fondazione Istituto Italiano di Tecnologia, Via Barsanti, 73010 Arnesano (Lecce), ITALY. E-mail: Andrea.Listorti@iit.it
[b] Center for Nano Science and Technology@Polimi, Istituto Italiano di Tecnologia, via G. Pascoli 70/3, 20133 Milano, Italy.
[c] Dept. of Physics, Politecnico di Milano, p.zza Leonardo da Vinci 32, Milano, Italy
[d] NNL – National Nanotechnology Laboratory, CNR Istituto Nanoscienze, Distretto Tecnologico, Via Arnesano 16, 73100 Lecce, Italy
[e] Dipartimento di Matematica e Fisica "E. De Giorgi", Universita' del Salento, Via per Arnesano, 73100 Lecce, Italy

† V.R and S.C. contributed equally to the work.

Electronic Supplementary Information (ESI) available: material synthesis, device preparation procedures, description of experimental setups, and additional figures. See DOI: 10.1039/c000000x/

1. B. O'Regan and M. Grätzel, *Nature*, 1991, **353**, 737–739.

2. L. M. Peter, *J. Phys. Chem. Lett.*, 2011, **2**, 1861–1867.

3. A. Hagfeldt, G. Boschloo, L. Sun, L. Kloo, and H. Pettersson, *Chem. Rev.*, 2010, **110**, 6595–6663.

4. I. Chung, B. Lee, J. He, R. P. H. Chang, and M. G. Kanatzidis, *Nature*, 2012, **485**, 486–9.

5. M. M. Lee, J. Teuscher, T. Miyasaka, T. N. Murakami, and H. J. Snaith, *Science*, 2012, **338**, 643–647.

6. H. S. Kim, C. R. Lee, J. H. Im, K. B. Lee, T. Moehl, A. Marchioro, S. J. Moon, R. Humphry-Baker, J. H. Yum, J. E. Moser, M. Grätzel, and N.-G. Park, *Sci. Rep.*, 2012, **2**, 591–597.

7. M. Liu, M. B. Johnston, and H. J. Snaith, *Nature*, 2013, **501**, 395–398.

8. J. Burschka, N. Pellet, S. J. Moon, R. Humphry-Baker, P. Gao, M. K. Nazeeruddin, and M. Grätzel, *Nature*, 2013, **499**, 316-319.

9. D. B. Mitzi, I. B. M. T. J. Watson, P. O. Box, Y. Heights, and D. Mitzi, *J. Mater. Chem.*, 2004, **14**, 2355–2365.

10. D. B. Mitzi, C. a Feild, Z. Schlesinger, and R. B. Laibowitz, *J. Solid State Chem.*, 1995, **114**, 159–163.

11. C. R. Kagan, *Science*, 1999, **286**, 945–947.

12. D. B. Mitzi, C. A. Felid, W. T. A. Harrison, and A. M. Guloy, *Nature*, 1994, **369**, 467–469.

13. A. Kojima, K. Teshima, Y. Shirai, and T. Miyasaka, *J. Am. Chem. Soc.*, 2009, **131**, 6050–6051.

14. J. H. Im, C. R. Lee, J. W. Lee, S. W. Park, and N. G. Park, *Nanoscale*, 2011, **3**, 4088–4093.

15. J. H. Heo, S. H. Im, J. H. Noh, T. N. Mandal, C.-S. Lim, J. A. Chang, Y. H. Lee, H. Kim, A. Sarkar, M. K. Nazeeruddin, M. Grätzel, and S. Il Seok, *Nat. Photonics*, 2013, 486-492.

16. J. H. Noh, S. H. Im, J. H. Heo, T. N. Mandal, and S. Il Seok, *Nano Lett.*, 2013, **13**, 1764–1769.

17. S. Colella, E. Mosconi, P. Fedeli, A. Listorti, F. Gazza, F. Orlandi, P. Ferro, T. Besagni, A. Rizzo, G. Calestani, G. Gigli, F. De Angelis, and R. Mosca, *Chem. Mater.*, 2013, **25**, 4613–4618.

18. L. Etgar, P. Gao, Z. Xue, Q. Peng, A. K. Chandiran, and B. Liu, *J. Am. Chem. Soc.*, 2012, **134**, 17396−17399.

19. W. A. Laban and L. Etgar, *Energy Environ. Sci.*, 2013, **6**, 3249.

20. M. Ball, j, M. M. Lee, A. Hey, and H. J. Snaith, *Energy Environ. Sci.*, 2013, **6**, 1739–1743.

21. A. Listorti, B. O'Regan, and J. R. Durrant, *Chem. Mater.*, 2011, **23**, 3381–3399.

22. S. E. Koops, B. C. O'Regan, P. R. F. Barnes, and J. R. Durrant, *J. Am. Chem. Soc.*, 2009, **131**, 4808–18.

23. J. H. Bang and P. V. Kamat, *ACS Nano*, 2009, **3**, 1467–1476.

24. B. O'Regan, J. R. Durrant, P. M. Sommeling, and N. J. Bakker, *J. Phys. Chem. C*, 2007, **111**, 14001–14010.

25. H. J. Snaith, A. Petrozza, S. Ito, H. Miura, and M. Grätzel, *Adv. Funct. Mater.*, 2009, **19**, 1810–1818.

26. G. Boschloo and A. Hagfeldt, *Chem. Phys. Lett.*, 2003, **370**, 381–386.

27. B. O'Regan and F. Lenzmann, *J. Phys. Chem. B*, 2004, **108**, 4342–4350.

28. L. Schmidt-Mende, U. Bach, R. Humphry-Baker, T. Horiuchi, H. Miura, S. Ito, S. Uchida, and M. Grätzel, *Adv. Mater.*, 2005, **17**, 813–815.

29. A. Listorti, I. López-Duarte, M. V. Martínez-Díaz, T. Torres, T. DosSantos, P. R. F. Barnes, and J. R. Durrant, *Energy Environ. Sci.*, 2010, **3**, 1573-1579.

30. A. Listorti, C. Creager, P. Sommeling, J. Kroon, E. Palomares, A. Fornelli, B. Breen, P. R. F. Barnes, J. R. Durrant, C. Law, and B. O'Regan, *Energy Environ. Sci.*, 2011, **4**, 3494 –3501.

31. S. D. Stranks, G. E. Eperon, G. Grancini, C. Menelaou, M. J. P. Alcocer, T. Leijtens, L. M. Herz, A. Petrozza, and H. J. Snaith, *Science.*, 2013, **342**, 341-344.

32. G. Xing, N. Mathews, S. Sun, S. S. Lim, Y. M. Lam, M. Gratzel, S. Mhaisalkar, and T. C. Sum, *Science.*, 2013, **342**, 344–347.

33. P. Docampo, J. M. Ball, M. Darwich, G. E. Eperon, and H. J. Snaith, *Nat. Commun.*, 2013, **4**, 2761-2766.

34. U. B. Cappel, E. a. Gibson, A. Hagfeldt, and G. Boschloo, *J. Phys. Chem. C*, 2009, **113**, 6275–6281.

35. H. S. Kim, I. Mora-Sero, V. Gonzalez-Pedro, F. Fabregat-Santiago, E. J. Juarez-Perez, N.-G. Park, and J. Bisquert, *Nat. Commun.*, 2013, **4**, 2242–2249.

36. U. B. Cappel, S. M. Feldt, J. Schöneboom, A. Hagfeldt, and G. Boschloo, *J. Am. Chem. Soc.*, 2010, **132**, 9096–101.

37. V. Roiati, E. Mosconi, A. Listorti, S. Colella, G. Gigli, and F. De Angelis, *Prep.*

38. D. Bi, L. Yang, G. Boschloo, A. Hagfeldt, and E. M. J. Johansson, *J. Phys. Chem. Lett.*, 2013, **4**, 1532–1536.

39. M. Westerling, C. Vijila, R. Österbacka, and H. Stubb, *Phys. Rev. B*, 2003, **67**, 195201.

40. A. Abrusci, S. D. Stranks, P. Docampo, H.-L. Yip, A. K.-Y. Jen, and H. J. Snaith, *Nano Lett.*, 2013, 3124–3128.

Broader context

The recent employment of self-assembling hybrid halide perovskites, in full solid sensitized solar cells, has signified a substantial advancement for third generation photovoltaic, allowing the achievement of record efficiencies up to 15% for low cost and stable devices. Interestingly perovskites are easy to process and their physical properties can be widely tuned through material composition and preparation condition variations. For these properties perovskites are ideal candidates as key constituents of photovoltaic devices. In this context, however, only few studies have been dedicated to the comprehension of photoinduced charge generation and transport. We report on a detailed spectroscopic investigation aiming at understanding the charge dynamics in $(CH_3NH_3)PbI_{3-x}Cl_x$ sensitized mesostructured solar cells. Through the analysis of model systems and devices, we suggest a peculiar working mechanism. A double path for charge transport is proposed, according to the experimental evidences, allowing the electron percolation in both TiO_2 and perovskite media. In the context of this rapidly expanding research front, our study aims to underline the need of a specific investigating approach and device design of perovskite-based devices, as they differ substantially from classical solid state dye sensitized devices.

Table of Contents

Evidences for complementary carriers percolation paths in halide perovskite-sensitized mesostructured solar cells